BAMS Article

Development of an Integrated Modeling Framework for Visibility and Air Quality Forecasting in Delhi

A. Jayakumar,[a] T. J. Anurose,[a] Shweta Bhati,[a] Margaret A. Hendry,[b] Garry Hayman,[c] Hamish Gordon,[d] Paul Field,[b] Saji Mohandas,[a] Heather Rumbold,[b] Prafull Yadav,[e] Narendra Gokul Dhangar,[e] Avinash Parde,[e] Sandeep Wagh,[e] Sachin Ghude,[e] Andrew N. Ross,[f] Daniel Smith,[g] Stephen Dorling,[g] John P. George,[a] V. S. Prasad,[a] and M. Ravichandran[h]

KEYWORDS:
Fog;
Visibility;
Forecast verification/skill;
Air quality;
Aerosol-cloud interaction

ABSTRACT: Rapid urbanization has subjected the megacities of developing countries to various environmental stresses. Delhi, a major Indian megacity, faces increasing urban stress leading to reduction in air quality and visibility. These challenges necessitate an integrated modeling framework to mitigate adverse environmental impacts on public health. Therefore, we have developed an advanced version of the high-resolution Delhi Model with Chemistry and aerosol framework (DM-Chem) at the National Centre for Medium Range Weather Forecasting (NCMRWF) under the Weather and Climate Science for Service Partnership India (WCSSP India) project. This collaborative initiative between India and the United Kingdom aims to provide real-time forecasts of visibility and fine particulate matter ($PM_{2.5}$) for Delhi and neighboring regions during the winter season. The DM-Chem framework is unique due to its detailed urban canopy scheme and realistic aerosol representation, making it well suited for city-scale forecasts. It is designed to predict extreme fog and pollution events in the winter season. Here, we discuss the major physical parameterization improvements for the model, along with its skill and deficiencies in predicting extreme events. Notably, irrigation effects on surrounding agricultural areas have significantly improved fog and visibility forecasts, but have degraded the wind forecasts. We demonstrate the applicability of this modeling framework to study aerosol–radiation interaction during fog holes and discuss its potential to be applied or adapted to other megacities worldwide.

SIGNIFICANCE STATEMENT: The capital city Delhi and, in general, many metropolitan cities of India often report high levels of particulate matter pollution especially during wintertime, often accompanied by episodes of dense fog. Air quality and visibility forecasting for an urban region is dependent upon many key model inputs other than emissions and meteorology. Realistic representation of the (i) city's local urban morphology, (ii) surface aerosols, and (iii) soil conditions impacted by irrigation activities has been found to significantly influence air quality and visibility prediction in Delhi and surrounding areas. This work aimed at providing a reliable air quality and visibility forecast for Delhi, which is crucial to minimize both health and economic losses.

DOI: 10.1175/BAMS-D-24-0194.1
Corresponding author: A. Jayakumar, jayakumar.a@nic.in, jkumar@ncmrwf.gov.in
Supplemental information related to this paper is available at the Journals Online website: https://doi.org/10.1175/BAMS-D-24-0194.s1.
Manuscript received 26 July 2024, in final form 19 December 2024, accepted 2 January 2025

AFFILIATIONS: [a] National Centre for Medium Range Weather Forecasting, Ministry of Earth Sciences, Noida, India; [b] Met Office, Exeter, United Kingdom; [c] U.K. Centre for Ecology and Hydrology, Wallingford, United Kingdom; [d] Department of Chemical Engineering and Center for Atmospheric Particle Studies, Carnegie Mellon University, Pittsburgh, Pennsylvania; [e] Indian Institute of Tropical Meteorology, Pune, India; [f] School of Earth and Environment, University of Leeds, Leeds, United Kingdom; [g] School of Environmental Sciences, University of East Anglia, Norwich, United Kingdom; [h] Ministry of Earth Sciences, New Delhi, India

1. Introduction

Urban areas are increasingly experiencing environmental stress, particularly with the rapid urbanization observed in developing countries. The occurrence of extreme weather events, such as poor air quality, heatwaves, and intense precipitation, emphasizes the need for precise modeling of urban processes and their feedback mechanisms across various scales. Urban environments cause different challenges, mainly in terms of urban land–atmospheric interaction, arising from the complex building structures and their material properties, and the atmospheric composition, that is the high density of emissions and strong concentration gradients across the urban area (Harrison 2018). Unlike the broader regional and global atmospheric systems, local meteorology plays a more substantial role in determining atmospheric concentrations and influencing chemical transformations in urban areas. Air pollution and humid environments cause visibility degradation and fog formation during winter months, posing another major environmental challenge in some cities. According to the World Health Organization, exposure to ambient (outdoor) air pollution results in 4.2 million deaths annually. Airborne pollutants can act as nuclei for water droplets, aggravating fog formation. These unique characteristics underscore the necessity for specialized attention to urban atmospheric chemistry at city-scale resolutions.

India's capital region Delhi has grown in urban area by around 28% in the last two decades (Salem et al. 2021), with a corresponding increase in population. During winter, Delhi and the surrounding regions frequently encounter widespread fog events and air pollution episodes. The extensive irrigated area surrounding Delhi acts as a significant local moisture source, while aerosol transport, stubble mass burning, and other contributing factors lead to elevated aerosol mass levels in the region during winter. The interplay of increasing urbanization, cold winter weather with moist background, and a large number of aerosols pose challenges in predicting fog and air pollution events over Delhi. Hence, an integrated approach that considers all these factors is necessary to address this issue and minimize exposure to adverse environmental conditions in order to safeguard public health (Ghude et al. 2016).

Separate model frameworks are frequently used to provide short-term solutions for urban challenges like worsening air quality, diminished visibility, or extreme cold waves. However, these approaches increase computational demands, resulting in higher costs and greater manpower requirements. The current article highlights the application of the Delhi Model with Chemistry and aerosol framework (DM-Chem) as an integrated approach to handle urban aerosol chemistry to provide real-time forecast of both visibility and $PM_{2.5}$ for Delhi and the neighboring regions during the winter period. DM-Chem includes a prognostic aerosol chemistry scheme representing a reduced number of chemical species. This configuration

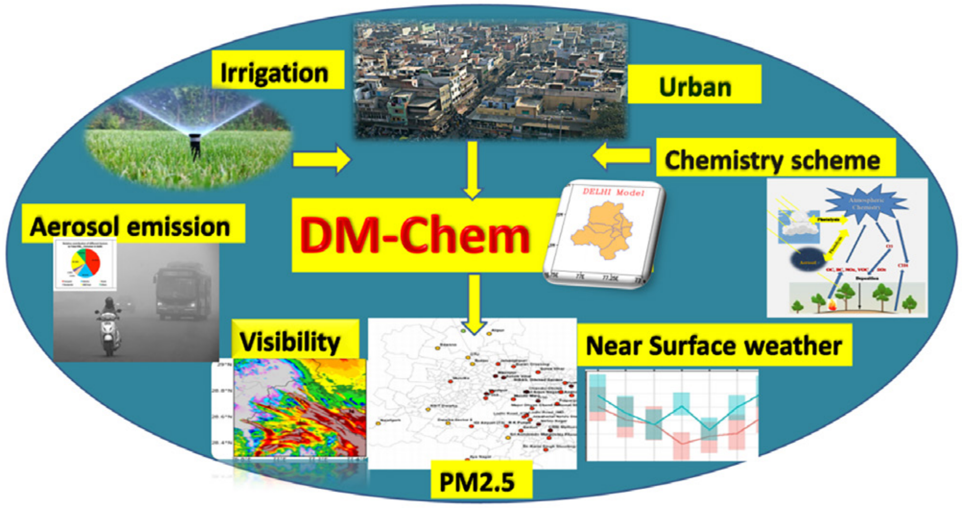

Fig. 1. Major modules in the DM-Chem1.0 (inward arrows) and the delivery products (outward arrows) from the model are schematically illustrated here.

is much less computationally expensive compared to full chemistry models, as discussed in Gordon et al. (2023). Together with this, a detailed urban scheme with the provision of local urban morphology, an advanced double-moment cloud microphysics scheme with aerosol–cloud coupling, a representation of the effects of irrigation, and a visibility scheme with prognostic aerosol (Fig. 1) make this system unique among other modeling approaches (Ghude et al. 2020; Parde et al. 2022; Tiwari et al. 2022). As an integrated system, DM-Chem addresses the complex interactions and feedback between urban environments, aerosols, vegetation, and cloud/fog microphysics, leading to more accurate forecasts of air quality and visibility. Given the prevalence of air pollution, urban flooding, and smog events in many cities (Wang et al. 2023), this kind of modeling system could prove beneficial for urban areas worldwide.

2. The evolution of the DM-Chem model

DM-Chem is a regional nested configuration of the Met Office Unified Model. It consists of an outer model domain with a 1.5-km grid spacing (extending from 73.61° to 80.6°E in the zonal direction and from 25.16° to 32.15°N in the meridional direction) and an inner nested model domain with a 330-m grid spacing (spanning from 76.65° to 77.55°E in the zonal direction and from 28.2° to 29.1°N in the meridional direction). DM-Chem has 80 vertical levels, with the first level positioned at 5 m above the ground and the top of the atmosphere set at 38.5 km. The initial version of DM-Chem, known as DM-Chem_baseline herein, was introduced by Jayakumar et al. (2021). The Joint U.K. Land Environment Simulator (JULES) is used as the land surface model in DM-Chem_baseline. To more accurately represent the urban stresses in a city like Delhi, DM-Chem_baseline has been developed into DM-Chem1.0. The primary differences between these versions include the incorporation of an enhanced urban canopy model, irrigation, and advanced cloud microphysics with aerosol interactions. Further details on the differences and similarities between the two versions are provided in Table A1 in appendix A. Details of the key components of DM-Chem1.0 are provided below.

a. Urban parameterization scheme. The urban canopy influences microscale meteorology and consequently pollutant dispersal. In DM-Chem1.0, a detailed two-tile urban scheme called the Met Office Reading Urban Surface Exchange Scheme (MORUSES) is used within the JULES land surface model. One type of tile represents rooftops, and the other street represents canyons (Best et al. 2011). This scheme replaces the one-tile urban scheme (a simple bulk representation for an urban area) used in DM-Chem_baseline (Theethai-Jacob et al. 2023, references within). MORUSES includes additional urban morphology parameters such as mean building height (H), canyon aspect ratio (H/W), and canyon width ratio (W/R), where W is the street canyon width and R is the combined length of canyon and roof. These are determined from Delhi specific empirical relationships derived from local urban morphology data of planar area index (the ratio of the land surface area occupied by buildings to the total urban area), frontal area index (the ratio of the surface area exposed to mean wind to the total urban area), and building height (further details are provided in appendix B). Incorporating MORUSES with appropriate local urban morphology improved the urban parameterization of DM-Chem (Theethai-Jacob et al. 2023).

b. Aerosol chemistry scheme and emission datasets. The aerosol and chemistry model of DM-Chem1.0, U.K. Chemistry and Aerosol (UKCA), represents the aerosol processes such as new particle formation, condensation and coagulation, and deposition using the Global Model of Aerosol Processes (GLOMAP)-mode aerosol scheme (Mann et al. 2010). The GLOMAP-mode aerosol scheme we use here simulates sulfate, black carbon, organic carbon, and sea spray aerosols distributed across five lognormal modes depending on their hygroscopicity and size. Dust is simulated by a separate sectional parameterization (Woodward 2001). The integration of UKCA with GLOMAP into high-resolution regional forecasting models is described by Gordon et al. (2023). DM-Chem_baseline includes a reduced chemistry mechanism within the UKCA chemistry scheme that matches the HadGEM3-GC3.1 climate model (Mulcahy et al. 2020). This reduced version uses prescribed monthly climatologies of the oxidants including ozone (O_3), hydroxyl radical (OH), nitrate radical (NO_3), hydroperoxyl radical (HO_2), and hydrogen peroxide (H_2O_2) to avoid the computational expense associated with full chemistry (Archibald et al. 2020). Further details of the chemistry scheme are provided in the supplemental material. The aerosols interact radiatively with the Suite of Community Radiative Transfer Codes based on Edwards and Slingo radiation scheme (Edwards and Slingo 1996) through the direct scattering and absorption process, those details are as outlined in Bellouin et al. (2013). Along with a high-resolution (300 m) inventory for anthropogenic emissions in the inner domain (Sahu et al. 2011), near-real-time fire emissions are also included. Fires are an important source of $PM_{2.5}$ during the October and November stubble burning season. The Global Fire Assimilation System emissions data are incorporated into DM-Chem1.0 once they become available (1-day delay mode), making the approximation that the emissions for the previous day will still be realistic 1 day later in the forecast. Dry deposition is the sink process for several trace gases and aerosols near the surface and depends on meteorological conditions, particle properties, and surface roughness. In the default dry deposition scheme of DM-Chem_baseline, all land surface types are classified as forest. It is improved in DM-Chem1.0 which identifies the dominant surface type, including the urban category, within each grid box (Zhang et al. 2001).

c. Coupling of the cloud microphysics with aerosol. DM-Chem1.0 includes Cloud Aerosol Interaction Microphysics (CASIM), a two-moment cloud microphysics scheme (Field et al. 2023) which considers the mass and number concentration of hydrometeors: rain, ice, snow, cloud droplet, and graupel. The aerosol chemistry model UKCA provides the aerosol number concentrations and sizes so that CASIM can calculate the number activated to cloud droplets (Gordon et al. 2020). The activation scheme in CASIM makes use of vertical velocity (w_{act}), humidity, and aerosol properties to compute the number concentration of droplets (Abdul-Razzak and Ghan 2000). During the dense fog events, cloud droplet number concentrations simulated by CASIM were lower than the observed cloud droplet number concentrations. This bias is improved by increasing w_{act} in the modified activation scheme of

DM-Chem1.0 (further details are discussed in appendix C). A new bimodal diagnostic cloud fraction parameterization is also a part of DM-Chem1.0 (van Weverberg et al. 2021). This parameterization identifies entrainment zones linked with strong temperature inversions. The bimodal skewed cloud diagnostic scheme is found to perform better than the unimodal, nonskewed scheme in DM-Chem_baseline.

d. Irrigation representation. DM-Chem_baseline exhibits a consistent dry humidity bias during the winter season over Delhi and the surrounding areas of the National Capital Region (NCR) of the country even after soil moisture is initialized through data assimilation (Theethai-Jacob et al. 2023). Studies indicate that an increase in irrigation impacts the weather (Thiery et al. 2020) and results in higher humidity levels during winter in this region (Choudhury and Bhattacharya 2021). Additionally, recent research suggests that additional soil moisture from irrigation affects the simulation of dense fog events over northern India (Smith et al. 2024). The JULES land surface model includes an irrigation parameterization that moistens soil moisture in the top two layers up to the critical soil moisture level (the point before which transpiration is impacted by water stress) (Best et al. 2011). In DM-Chem1.0, the irrigation scheme has been modified such that irrigated surface tiles are further moistened to saturation point. The saturation point is chosen to be consistent with the flood irrigation practice in the region. Irrigation is applied to tiles containing grass types at every model time step, as depicted in Fig. 1 in the online supplemental material.

e. Visibility parameterization. The DM-Chem_baseline visibility diagnostic is based on the extinction coefficient that is dependent on relative humidity and a prognostic aerosol content (Clark et al. 2008; Jayakumar et al. 2021). This approach accounts for the aerosol mass and aerosol number from GLOMAP mode in UKCA. Specifically, the aerosol mass and number is computed from the Aitken, accumulation, coarse soluble, and Aitken insoluble modes.

3. Potential of DM-Chem1.0 to predict urban stresses

In the winter months, Delhi and its surrounding regions experience weather extremes, primarily because of fog and air quality. We explored the potential of DM-Chem1.0 for simulating these events, focusing on January 2023, as historical data show that this month typically experiences the highest frequency of dense fog events in the Delhi area (Kulkarni et al. 2019). Additionally, severe air pollution episodes were also observed during this period in 2023.

a. Near-surface weather. Accurate simulation of minimum temperature is vital for fog forecasting, particularly for radiation fog cases, the most prevalent dense fog type over Delhi (Smith et al. 2023). DM-Chem1.0 accurately captures the diurnal evolution and minimum values of air temperature throughout the month (Figs. 2a,d). Incorporation of the urban scheme, MORUSES (Theethai-Jacob et al. 2023), in DM-Chem1.0 leads to improve near-surface air temperatures during the night and early morning hours. Furthermore, the increased soil moisture from irrigation in DM-Chem1.0 enhances the soil's heat capacity, latent heat fluxes, and reduces sensible heat fluxes leading to lower near-surface temperatures (Chen and Jeong 2018). Consequently, near-surface air temperatures tend to be cooler during the day in DM-Chem1.0.

Near-surface humidity serves as another important parameter to initiate fog formation. While there is some overestimation of daily averaged relative humidity (RH) on certain dates (15–20 January) (Fig. 2b), DM-Chem1.0 generally outperforms DM-Chem_baseline. It is noteworthy that DM-Chem1.0 accurately simulates the diurnal evolution of RH, which could be attributed to representing irrigation (Fig. 2e). The wind speed in DM-Chem1.0 is

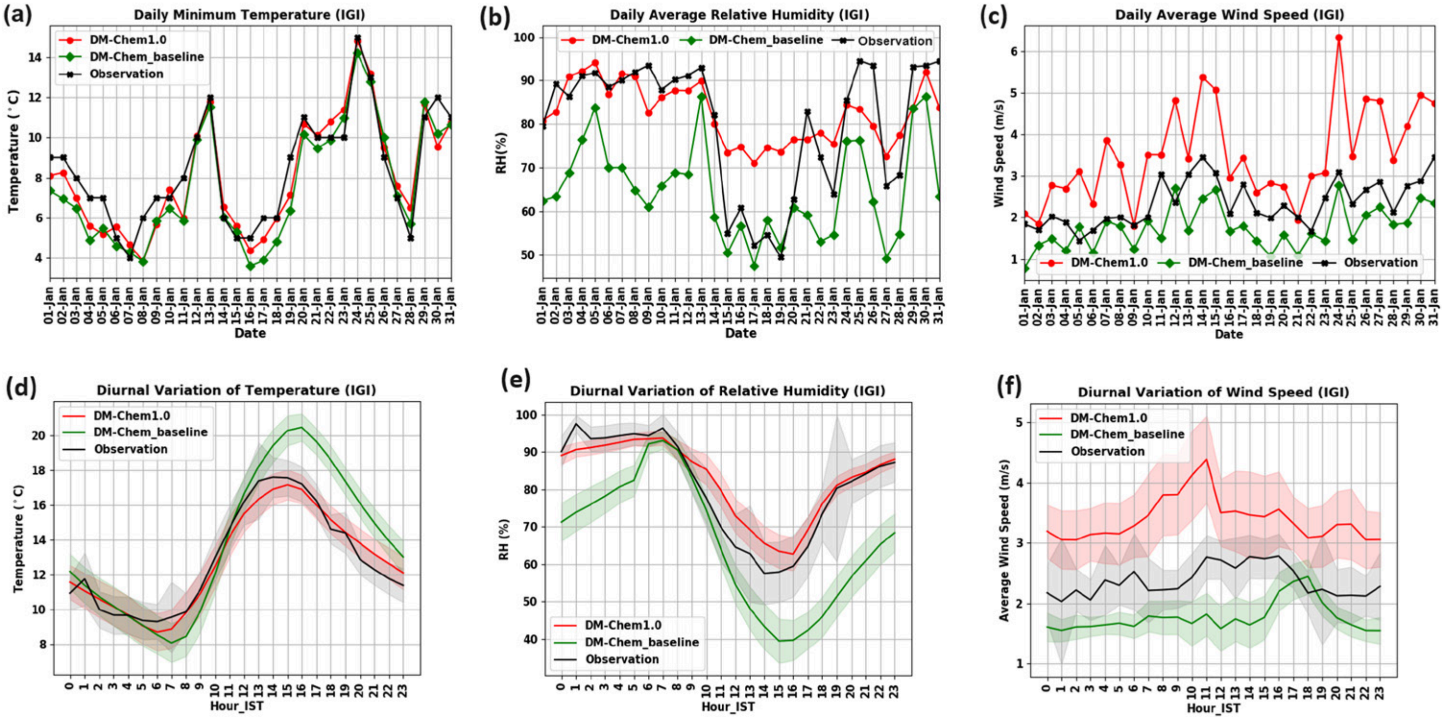

Fig. 2. Time series of observed and simulated (a) daily minimum air temperature (1.5 m), (b) daily average RH (1.5 m), and (c) daily average wind speed (10 m) and the mean diurnal variation of (d) temperature (1.5 m), (e) RH (1.5 m), and (f) wind speed (10 m) with standard deviation (shading) at IGI Airport (28.57°N, 77.12°E, as indicated in Fig. 4) across January 2023.

predominantly overestimated. Nevertheless, the diurnal evolution of wind speed illustrates a better pattern in DM-Chem1.0 (Figs. 2c,f) compared to DM-Chem_baseline. The changes in wind speed in DM-Chem1.0 primarily arise from including the urban scheme, MORUSES and irrigation (supplemental Fig. 3). The overestimation of wind speed needs further investigation and improvement.

b. Fog and air quality. Given that fog and air quality are the primary weather concerns, visibility and particulate matter (specifically $PM_{2.5}$) are the key factors to consider. The DM-Chem_baseline model tends to underestimate visibility, often falsely predicting dense fog conditions (visibility < 0.2 km) for most days of the month (Fig. 3a). However, with the revised visibility parameterizations in DM-Chem1.0, significant improvement is evident in the visibility forecast across various fog conditions: dense (<0.2 km) on 11 out of 12 days, moderate (<0.5 km) on 3 out of 5 days, and shallow fog (<1.0 km) on 8 out of 12 days. The diurnal evolution of visibility from DM-Chem1.0 shows significant improvement during the night and early morning hours (Fig. 3c). It is important to note that runway visual range observations at Indira Gandhi International (IGI) Airport (location is depicted in Fig. 4) are restricted to 2.5 km, which limits the evaluation of visibility simulations during daytime on clear days.

It can be seen in Fig. 3b that DM-Chem1.0 performs well for daily average $PM_{2.5}$ concentrations. In particular, the model captures the concentration peak during the dense fog event of 8–9 January 2023, though there is an underestimation in general. The daily average $PM_{2.5}$ concentrations estimated by DM-Chem1.0 are higher compared to those estimated by DM-Chem_baseline and demonstrate closer agreement with the observed concentrations. The diurnal variation of observed $PM_{2.5}$ concentrations (Fig. 3d) shows a bimodal distribution with two peaks observed in the morning and evening hours. Although the diurnal evolution of $PM_{2.5}$ from DM-Chem1.0 is relatively better during evening and nighttime hours, both simulations exhibit overestimation in the early morning hours and marked underestimation during daytime. Identifying the exact reasons for these discrepancies is challenging due to the

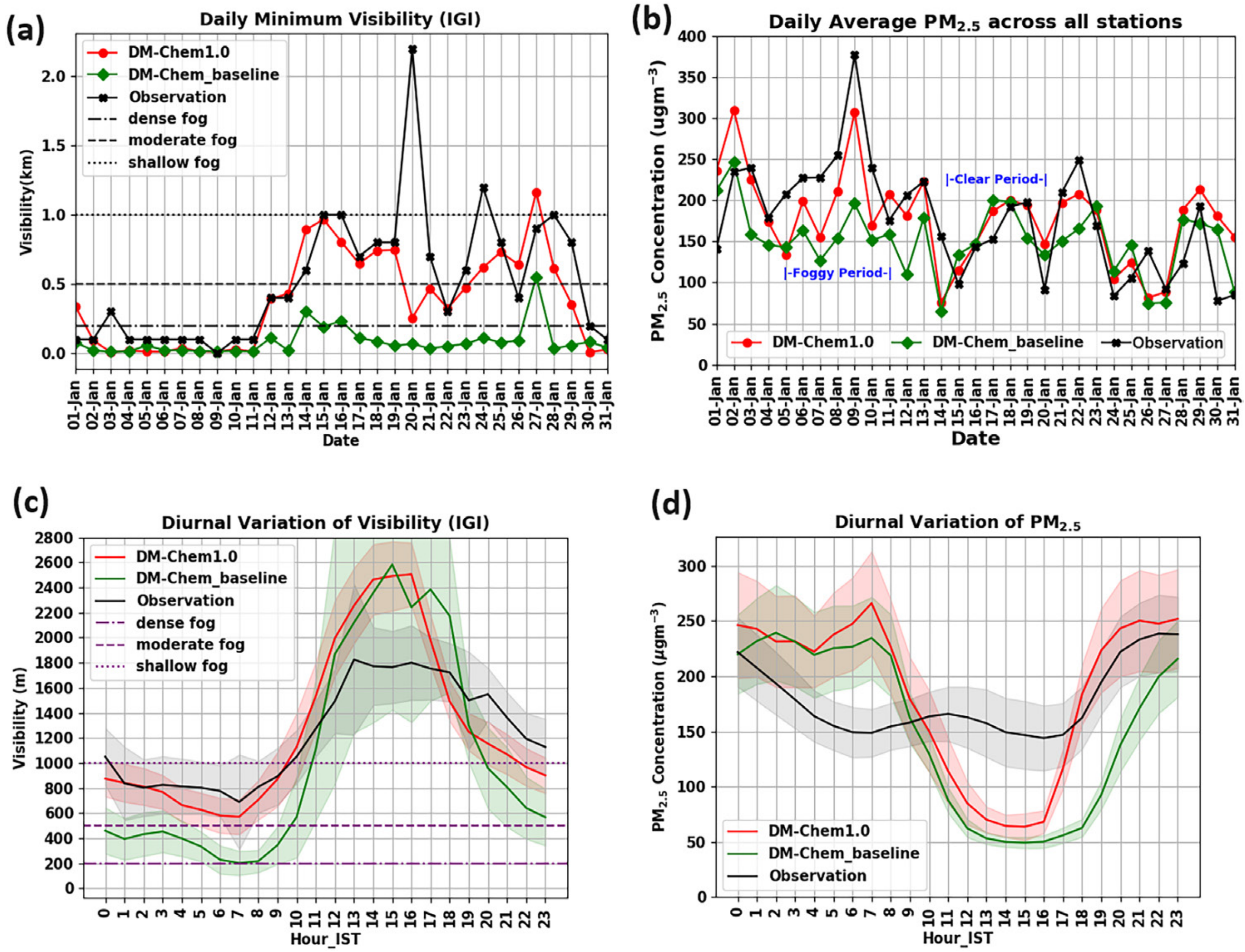

Fig. 3. Time series of (a) daily minimum visibility (1.5 m) over IGI and (b) daily average $PM_{2.5}$ across all major stations in Delhi and the mean diurnal variation of (c) visibility (1.5 m) over IGI (d) $PM_{2.5}$ across all major stations in Delhi with standard deviation (shading) for the winter month of January 2023.

nonlinear relationship between pollutant concentration and controlling factors arising from the complex chemistry, local emission, and atmospheric dynamics. The amplified particle growth caused by the higher humidity levels lead to the improvement of $PM_{2.5}$ in the evening and nighttime hours as observed in earlier studies (e.g., Gunthe et al. 2021).

c. Air quality index. An air quality index (AQI) serves as an indicator developed by government agencies to inform the public about the current level of air pollution. AQI comprises six categories: good, satisfactory, moderate, poor, very poor, and severe. The AQI in India is based on eight pollutants: PM_{10}, $PM_{2.5}$, nitrogen dioxide (NO_2), sulfur dioxide (SO_2), carbon monoxide (CO), O_3, ammonia (NH_3), and lead (Pb). The concentration values of $PM_{2.5}$ associated with each AQI category are stipulated by the Central Pollution Control Board of India (Table S2). Figure 4 shows the average AQI computed from observations and simulations utilizing $PM_{2.5}$ data at various monitoring stations in Delhi during January 2023. Among the 39 stations, 37 register very poor and severe AQI levels according to observed data, whereas DM-Chem1.0 predicts very poor and severe AQI for 31 stations.

d. Statistical evaluation of DM-Chem1.0. The performance of the model for simulated near-surface variables is assessed statistically using root-mean-square error (RMSE) and the

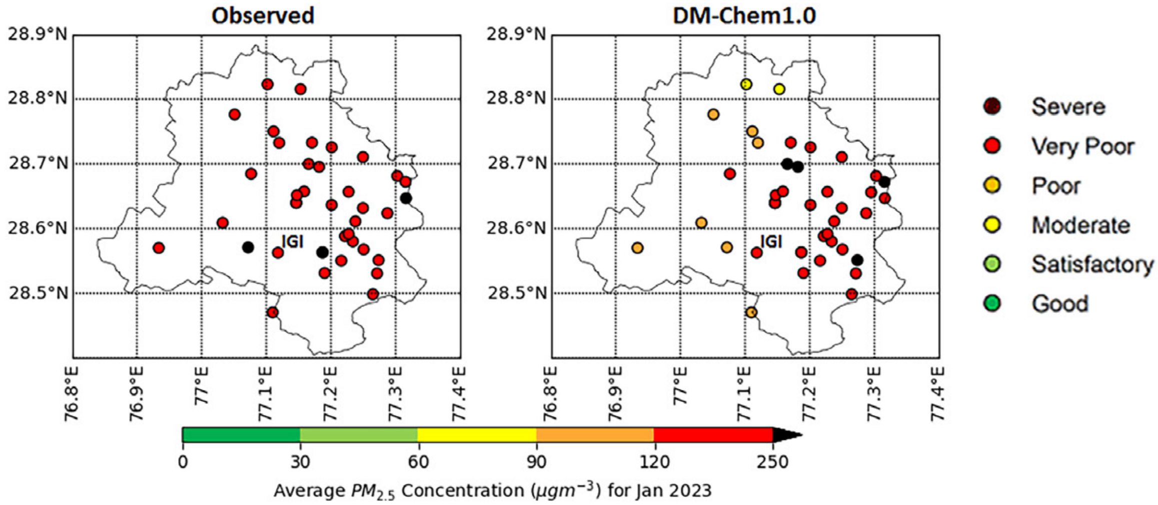

Fig. 4. AQI for the month of January 2023 for various stations in Delhi (boundary shown).

index of agreement (IoA) (Willmott 1981). The index of agreement is a standardized metric for quantifying the degree of prediction error and is the ratio of the mean-square error and the potential error. Potential error is defined as the sum of the squared absolute differences between the predicted values and the mean of the observed values, as well as between the observed values and their mean. IoA ranges from 0 to 1, where higher values indicate that the modeled values better agree with the observations.

A decrease in RMSE and an increase in IoA are observed for both temperature and RH from DM-Chem_baseline to DM-Chem1.0, as shown in Table 1. Statistical evaluation of RMSE and IoA for hourly visibility during nighttime (1930–0630 LT), as estimated by both simulations, also demonstrates improvement with DM-Chem1.0. However, the wind statistics worsen in DM-Chem1.0. As shown in supplemental Fig. 3, wind speed over IGI increased after irrigation. Although this location is not an irrigated area, studies (Lunel et al. 2024; Smith et al. 2024) report that irrigation-induced breezes can occur from irrigated to semiarid areas.

Additionally, Table 2 presents various metrics for comparing the performance of the two model configurations for categorical forecast evaluation in terms of accuracy (A), false alarm rate (FAR), and critical success index (CSI) or threat score for visibility (Jolliffe and Stephenson 2003). Higher values of A and CSI, along with lower values of FAR, indicate improved model performance. DM-Chem1.0 has better accuracy and lower FAR, especially for the prediction of moderate and dense fog events. The CSI is also improved in DM-Chem1.0 for moderate and dense fog cases, where visibility is less than 500 m, compared to the baseline configuration. Visibility in DM-Chem1.0 is controlled by both RH and aerosols. Hence, improvement in both RH and aerosol prediction would likely

Table 1. Discrete statistics for model performance for hourly values of temperature, RH, visibility, and wind speed at IGI Airport and $PM_{2.5}$ averaged for all monitoring stations over Delhi for the period of 1–31 Jan 2023. (V0: DM-Chem_baseline; V1: DM-Chem1.0).

Statistics →	RMSE		IoA	
Parameter ↓	V0	V1	V0	V1
Temp (1.5 m)	2.97°C	1.81°C	0.89	0.94
RH	22.93%	14.11%	0.76	0.82
Visibility (night)	0.86 km	0.60 km	0.59	0.68
Wind speed (10 m)	1.13 m s^{-1}	1.96 m s^{-1}	0.61	0.53
$PM_{2.5}$	178 μgm^{-3}	120 μgm^{-3}	0.41	0.60
$PM_{2.5}$ (daily average)	68 μgm^{-3}	62 μgm^{-3}	0.58	0.71

Table 2. Categorical statistics for (i) visibility (IGI Airport, 1930–0630 h local time) and (ii) $PM_{2.5}$ (daily average from all stations over Delhi) based on AQI category for the period of 1–31 Jan 2023. (V0: DM-Chem_baseline; V1: DM-Chem1.0).

	A (%) (ideal: 100%)		FAR (ideal: 0)		CSI (ideal: 1)	
(i) Visibility↓ Skill→	V0	V1	V0	V1	V0	V1
Visibility ≤ 1000 m	74.49	74.49	0.24	0.19	0.73	0.71
Visibility ≤ 500 m	59.18	77.55	0.53	0.32	0.47	0.54
Visibility ≤ 200 m	56.12	80.61	0.68	0.31	0.27	0.37
(ii) AQI↓ Skill→	A (%)		FAR		CSI	
Poor	70.86	76.53	0.90	0.81	0.05	0.10
Very poor	49.19	50.09	0.43	0.42	0.29	0.31
Severe	77.25	72.12	0.75	0.76	0.14	0.17

improve the visibility estimations as well. The model's accuracy and FAR in predicting AQI show improvement compared to the baseline for all categories, except for the severe AQI category. CSI for all AQI categories demonstrates improvement in DM-Chem1.0 compared to DM-Chem_baseline.

e. Application of DM-Chem1.0 for aerosol–radiation interaction: A fog hole event. The effect of aerosol urban feedback is studied using DM-Chem1.0 to understand the mechanism behind fog holes over Indo-Gangetic Plain (IGP) of India. Detailed explanations and technical results of this study are available in Anurose et al. (2024). Fog holes, isolated patches within widespread fog, are frequently observed over cities like Delhi, India. The reason behind this occurrence was mainly attributed to the urban heat island effect (Gautam and Singh 2018). It is observed that these holes can vary in size and are neither embedded in the same region nor always coincide with the urban areas. Compared to the well-defined fog hole over the urban area, the rural fog hole identified is a wider region in which the fog dissipates earlier. It appears like an open patch in an extensive fog cover which is sometimes not even surrounded by fog.

Using DM-Chem1.0, two widespread dense fog hole events are studied: one on 22 January 2016, over an urban area (not shown here but in Anurose et al. 2024), and another on 23 December 2019, over a rural area in the IGP region. These cases were chosen based on fog hole formation and satellite coverage, with details reported in earlier literature (Theethai-Jacob et al. 2023; Jayakumar et al. 2021). Figure 5 shows the spatial distribution of vertically integrated cloud liquid water and visibility at 2 m (t + 29-h forecast) for the control (CTRL) and aerosol absorption of radiation off (ABSOFF) experiments for 23 December 2019, rural fog hole case, from DM-Chem1.0. The CTRL and ABSOFF experiments differ only in terms of aerosol absorption, which is turned off in the latter. Results are compared with the Indian National Satellite System three-dimensional image fog product [not shown here but in Anurose et al. (2024), available at half-hourly intervals] and liquid water path from MODIS satellite observations (around 0500 UTC over the domain). The liquid water path is calculated from cloud physical parameters such as cloud effective radius and optical depth from MODIS (Jayakumar et al. 2021).

Numerical simulations using DM-Chem1.0 demonstrate that aerosol–radiation interaction leads to fog holes over both urban and rural regions. In urban fog holes, anthropogenic aerosols and associated aerosol–radiation interaction predominantly dominate the urban heat island effect, while in rural fog holes, aerosol absorption due to aerosol–radiation interaction is the main controlling factor. The differences in the characteristics of these fog holes, including their onset, duration, and dissipation, are addressed in Anurose et al. (2024).

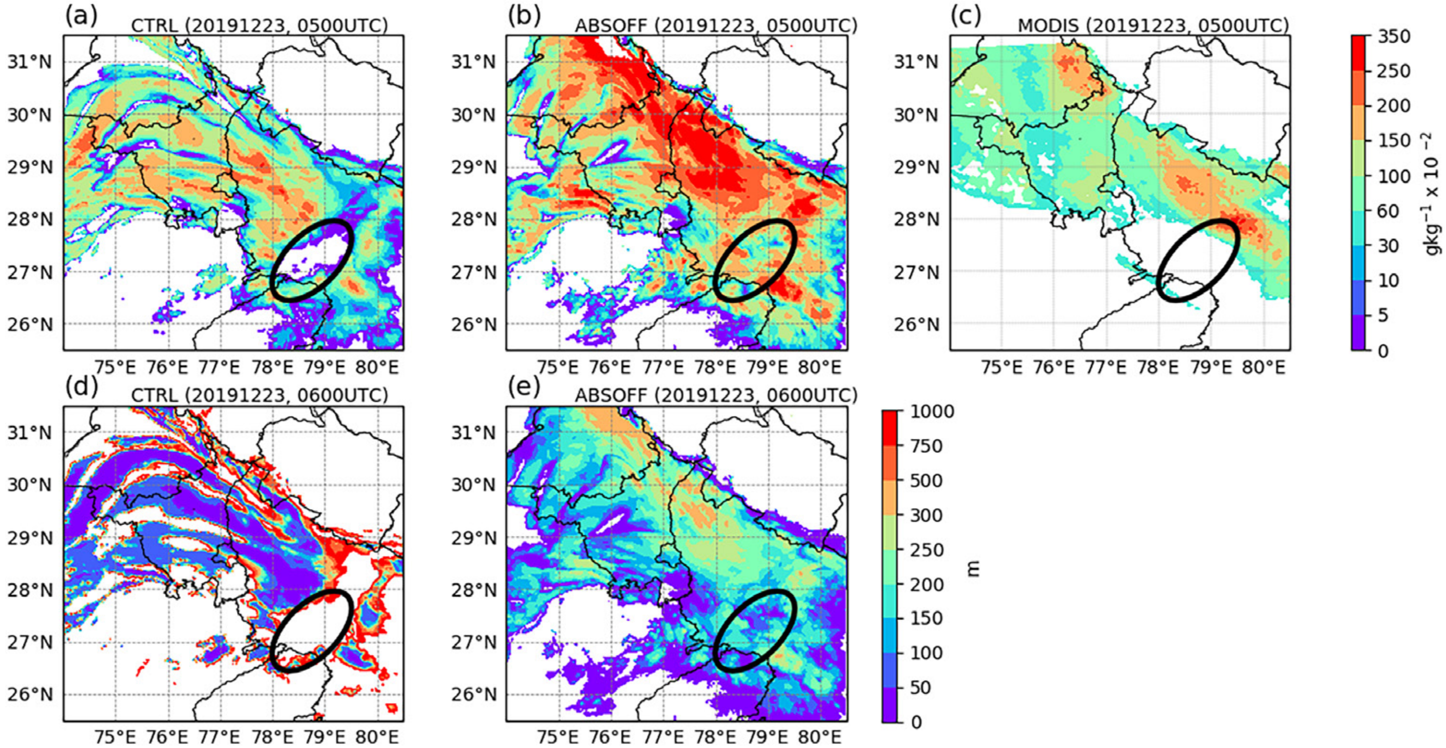

Fig. 5. Spatial distribution of (a) vertically integrated cloud liquid water and (d) 2-m visibility for CTRL experiments and (b),(e) for ABSOFF experiments, respectively, at 0500 UTC on 23 Dec 2019 (t + 29-h forecast) from DM-Chem1.0, along with (c) liquid water path from MODIS. Rural fog hole is indicated by black oval. Visibility values greater than 1000 m are masked.

4. Discussion and conclusions

Most developing countries face common challenges in mitigating urban air pollution, flooding, and visibility issues while advancing sustainable development. Additionally, each city faces unique issues, such as unorganized development, heavy aerosol loading, moist environments, and local emissions. This research highlights the various challenges in the integrated modeling system for a megacity in India and emphasizes the need to incorporate city-specific complexities for accurate simulation of urban stresses. The high-resolution modeling system, DM-Chem1.0, with advanced cloud microphysics, a detailed urban scheme including local urban morphology, a prognostic reduced chemistry aerosol scheme, and an irrigation representation, addresses these complexities to some extent, enabling more accurate predictions of urban stresses such as air quality and fog. The model performance for $PM_{2.5}$ and visibility is substantially improved in DM-Chem1.0 compared to DM-Chem_baseline. The real-time product of DM-Chem1.0 for the winter season is available on the Indian Institute of Tropical Meteorology (IITM) web server (https://ews.tropmet.res.in/analysis.php). There is considerable potential to apply this integrated modeling framework, incorporating additional city-specific complexities if any, to various megacities in developing countries experiencing similar urban stress issues.

One of the issues identified in the current study is the overestimation of simulated surface winds compared to the observed calm wind conditions that generally prevailed during this period (supplemental Fig. 2). This is likely due to irrigation-induced breezes from the irrigated area to the semiarid area due to strong surface heterogeneities, as reported in earlier studies (Lunel et al. 2024; Smith et al. 2024). There is scope to refine the current irrigation representation in the model by incorporating the type of irrigation, water control, and moistening based on irrigation maps. Additionally, a detailed study of irrigation-induced breezes gives a wide scope to hopefully understand the city scale flow and to improve the near-surface wind simulations.

Another challenge is in the prediction of diurnal evolution of $PM_{2.5}$. The simulated $PM_{2.5}$ pattern closely follows meteorology and the boundary layer evolution, showing a decrease during the daytime when boundary layer peaks and an increase at night when shallow boundary layer persist (supplemental Fig. 3), whereas observations show a bimodal peak which is more linked to morning rush hours and nighttime local emissions (Chen et al. 2020). Although monthly mean local emission climatologies were provided in the model, the need for diurnal factors is evident. Introducing assimilation of local aerosols could also improve this aspect, and further research is required.

The interaction between aerosols and fog/clouds has become a highly active area of research.

DM-Chem1.0 demonstrates its potential in studying aerosol–radiation–fog/cloud interactions. The role of aerosol absorption in fog hole areas underscores the need for more observational evidence of absorbing aerosols, which is currently lacking over the IGP region.

Acknowledgments. The work is supported by the research grant of NCMRWF, Ministry of Earth Sciences (MoES), and conducted through WCSSP India, a collaborative initiative between MoES and the Met Office, U.K. We thank MODIS teams for the level 1b and level 2 data products and the Indian Meteorological Department (IMD) for providing the SYNOP data. GH acknowledges the support of the NERC National Capability Awards: UKESM NE/V01319X/1 and TerraFIRMA NE/W004895/1.

Data availability statement. Due to intellectual property right restrictions, the Met Office Unified Model is available for use under license for NCMRWF, being a core partner. For further information on how to apply for a license, see http://www.metoffice.gov.uk/research/modelling-systems/unified-model. The data used to initialize the DM-Chem1.0 are from METUM data which is cited in Jayakumar et al. (2021). The MODIS liquid water path datasets were acquired from the Level 1 and Atmosphere Archive and Distribution System (LAADS) Distributed Active Archive Center (DAAC), located in the Goddard Space Flight Center in Greenbelt, Maryland (https://ladsweb.nascom.nasa.gov/). The SYNOP data are available from the Indian Meteorological Department (http://aws.imd.gov.in/) on request.

APPENDIX A
DM-Chem_baseline and DM-Chem1.0

The differences and similarities between DM-Chem_baseline and DM-Chem1.0 are summarized in Table A1.

Table A1. Major physics details for the two versions of the DM-Chem used in the present study.

Details	DM-Chem_baseline	DM-Chem1.0
Cloud microphysics	Single-moment scheme (Wilson and Ballard 1999)	Double-moment CASIM microphysics scheme (Field et al. 2023)
Cloud fraction scheme	Diagnostic scheme (Smith 1990)	Bimodal cloud scheme (van Weverberg et al. 2021)
Urban parameterization	Simple one-tile scheme	Detailed urban scheme, MORUSES with local morphology (Theethai-Jacob et al. 2023)
Irrigation representation	Not included	Irrigation is based on the irrigation scheme from the JULES land surface model. Soil moisture is saturated over irrigated grasslands
Aerosol scheme	GLOMAP mode (Mann et al. 2010)	Same as in the DM-Chem_baseline
Dry deposition treatment	Noninteractive and only one surface type is used	Meteorological dependent Wesely-type scheme (Wesely 1989), considered for all the land surface categories.
Initialization and boundary condition	Meteorological and chemistry/aerosol initial and boundary condition using NCMRWF operational setup outlined in Jayakumar et al. (2021)	Same as in the DM-Chem_baseline
Emission	EDGAR and SAFAR inventory for 1.5-km and 330-m domain, respectively	Same as in the DM-Chem_baseline
Visibility parameterization	Visibility diagnostic approach based on Jayakumar et al. (2021). Aerosol number concentration is derived from the accumulation modes	Similar to the DM-Chem_baseline, except that the aerosol number concentration is derived from the Aitken, accumulation, and coarse modes

APPENDIX B

Urban Parameterization: New Empirical Relationship

A new empirical relationship is established for the urban parameterization scheme, MORUSES scheme between urban fraction (f_u) and the input parameters frontal area index λ_f, planar area index λ_p, and building height H from the local urban morphology of Delhi (Theethai-Jacob et al. 2023). The urban data from the European Space Agency Climate Change Initiative Land Cover are converted into a fractional map within the JULES model using a cross-walking table.

$$\lambda_p = 0.6121 f_u^2 + 0.2179 f_u + 0.004\ldots, \tag{B1}$$

$$\lambda_f = -4.7883 f_u^6 + 14.447 f_u^5 - 16.833 f_u^4 + 9.5361 f_u^3 - 2.7637 f_u^2 + 0.4124 f_u + 0.0014, \tag{B2}$$

$$H = -58.974 f_u^6 + 305.3 f_u^5 - 449.15 f_u^4 + 252.251 f_u^3 - 42.235 f_u^2 + 0.2127 f_u + 1.5192\ldots. \tag{B3}$$

APPENDIX C

Improvement to Activation Scheme in CASIM

Activation scheme in Cloud Aerosol Interaction Microphysics (CASIM) makes use of vertical velocity (w_{act}) for the computation of the number concentration of droplets activated (Abdul-Razzak and Ghan 2000). The w_{act} is obtained by adding the resolved vertical velocity (w) to a scaled subgrid turbulent kinetic energy (TKE) (Field et al. 2023) according to $w_{\mathrm{act}} = w + c\sqrt{\mathrm{tke}}$. The value of c is 1 in the baseline version of CASIM. However, during dense fog events, cloud droplet number concentrations (CDNCs) simulated by CASIM were lower than the observed CDNC. The value of TKE is critical and increases during the optically thick phase of the fog (Dhangar et al. 2021). Therefore, to include the impact of unresolved vertical velocity in the simulation of droplet concentrations during dense fog, the activation velocity is increased by keeping $c = 2$ after iterations based on the observed CDNC.

References

Abdul-Razzak, H., and S. J. Ghan, 2000: A parameterization of aerosol activation: 2. Multiple aerosol types. *J. Geophys. Res.*, **105**, 6837–6844, https://doi.org/10.1029/1999JD901161.

Anurose, T. J., A. Jayakumar, M. Sandhya, H. Gordon, S. Aryasree, S. Mohandas, S. Bhati, and V. S. Prasad, 2024: Unraveling the mechanism of the holes in the blanket of fog over the Indo-Gangetic plains: Are they driven by urban heat islands or aerosol? *Geophys. Res. Lett.*, **51**, e2023GL107252, https://doi.org/10.1029/2023GL107252.

Archibald, A. T., and Coauthors, 2020: Description and evaluation of the UKCA stratosphere–troposphere chemistry scheme (StratTrop vn 1.0) implemented in UKESM1. *Geosci. Model Dev.*, **13**, 1223–1266, https://doi.org/10.5194/gmd-13-1223-2020.

Bellouin, N., G. W. Mann, M. T. Woodhouse, C. Johnson, K. S. Carslaw, and M. Dalvi, 2013: Impact of the modal aerosol scheme GLOMAP-mode on aerosol forcing in the Hadley Centre Global Environmental Model. *Atmos. Chem. Phys.*, **13**, 3027–3044, https://doi.org/10.5194/acp-13-3027-2013.

Best, M. J., and Coauthors, 2011: The Joint UK Land Environment Simulator (JULES), model description – Part 1: Energy and water fluxes. *Geosci. Model Dev.*, **4**, 677–699, https://doi.org/10.5194/gmd-4-677-2011.

Chen, X., and S.-J. Jeong, 2018: Irrigation enhances local warming with greater nocturnal warming effects than daytime cooling effects. *Environ. Res. Lett.*, **13**, 024005, https://doi.org/10.1088/1748-9326/aa9dea.

Chen, Y., O. Wild, L. Conibear, L. Ran, J. He, L. Wang, and Y. Wang, 2020: Local characteristics of and exposure to fine particulate matter ($PM_{2.5}$) in four Indian megacities. *Atmos. Environ.*, **5**, 100052, https://doi.org/10.1016/j.aeaoa.2019.100052.

Choudhury, I., and B. K. Bhattacharya, 2021: A baseline estimate of regional agricultural water demand from GEO-LEO satellite observations. *Geocarto Int.*, **37**, 3416–3440, https://doi.org/10.1080/10106049.2020.1856198.

Clark, P. A., S. A. Harcourt, B. Macpherson, C. T. Mathison, S. Cusack, and M. Naylor, 2008: Prediction of visibility and aerosol within the operational Met Office Unified Model. I: Model formulation and variational assimilation. *Quart. J. Roy. Meteor. Soc.*, **134**, 1801–1816, https://doi.org/10.1002/qj.318.

Dhangar, N. G., and Coauthors, 2021: On the conditions for onset and development of fog over New Delhi: An observational study from the WiFEX. *Pure Appl. Geophys.*, **178**, 3727–3746, https://doi.org/10.1007/s00024-021-02800-4.

Edwards, J. M., and A. Slingo, 1996: Studies with a flexible new radiation code. I: Choosing a configuration for a large-scale model. *Quart. J. Roy. Meteor. Soc.*, **122**, 689–719, https://doi.org/10.1002/qj.49712253107.

Field, P. R., and Coauthors, 2023: Implementation of a double moment cloud microphysics scheme in the UK Met Office regional numerical weather prediction model. *Quart. J. Roy. Meteor. Soc.*, **149**, 703–739, https://doi.org/10.1002/qj.4414.

Gautam, R., and M. K. Singh, 2018: Urban heat island over Delhi punches holes in widespread fog in the Indo-Gangetic Plains. *Geophys. Res. Lett.*, **45**, 1114–1121, https://doi.org/10.1002/2017GL076794.

Ghude, S. D., and Coauthors, 2016: Premature mortality in India due to $PM_{2.5}$ and ozone exposure. *Geophys. Res. Lett.*, **43**, 4650–4658, https://doi.org/10.1002/2016GL068949.

——, and Coauthors, 2020: Evaluation of $PM_{2.5}$ forecast using chemical data assimilation in the WRF-Chem model: A novel initiative under the Ministry of Earth Sciences Air Quality Early Warning System for Delhi, India. *Curr. Sci.*, **118**, 1803–1815, https://doi.org/10.18520/cs/v118/i11/1803-1815.

Gordon, H., and Coauthors, 2020: Development of aerosol activation in the double-moment Unified Model and evaluation with CLARIFY measurements. *Atmos. Chem. Phys.*, **20**, 10 997–11 024, https://doi.org/10.5194/acp-20-10997-2020.

——, and Coauthors, 2023: NUMAC: Description of the Nested Unified Model with aerosols and chemistry, and evaluation with KORUS-AQ data. *J. Adv. Model. Earth Syst.*, **15**, e2022MS003457, https://doi.org/10.1029/2022MS003457.

Gunthe, S. S., and Coauthors, 2021: Enhanced aerosol particle growth sustained by high continental chlorine emission in India. *Nat. Geosci.*, **14**, 77–84, https://doi.org/10.1038/s41561-020-00677-x.

Harrison, R. M., 2018: Urban atmospheric chemistry: A very special case for study. *npj Climate Atmos. Sci.*, **1**, 20175, https://doi.org/10.1038/s41612-017-0010-8.

Jayakumar, A., H. Gordon, T. Francis, A. A. Hill, S. Mohandas, B. S. Sandeepan, A. K. Mitra, and G. Beig, 2021: Delhi Model with Chemistry and aerosol framework (DM-Chem) for high-resolution fog forecasting. *Quart. J. Roy. Meteor. Soc.*, **147**, 3957–3978, https://doi.org/10.1002/qj.4163.

Jolliffe, I. T., and D. B. Stephenson, 2003: *Forecast Verification: A Practitioners Guide in Atmospheric Science.* John Wiley and Sons, 254 pp.

Kulkarni, R., R. K. Jenamani, P. Pithani, M. Konwar, N. Nigam, and S. D. Ghude, 2019: Loss to aviation economy due to winter fog in New Delhi during the winter of 2011–2016. *Atmosphere*, **10**, 198, https://doi.org/10.3390/atmos10040198.

Lunel, T., A. A. Boone, and P. Le Moigne, 2024: Irrigation strongly influences near-surface conditions and induces breeze circulation: Observational and model-based evidence. *Quart. J. Roy. Meteor. Soc.*, **150**, 2798–2819, https://doi.org/10.1002/qj.4736.

Mann, G. W., K. S. Carslaw, D. V. Spracklen, D. A. Ridley, P. T. Manktelow, M. P. Chipperfield, S. J. Pickering, and C. E. Johnson, 2010: Description and evaluation of GLOMAP-mode: A modal global aerosol microphysics model for the UKCA composition-climate model. *Geosci. Model Dev.*, **3**, 519–551, https://doi.org/10.5194/gmd-3-519-2010.

Mulcahy, J. P., and Coauthors, 2020: Description and evaluation of aerosol in UKESM1 and HadGEM3-GC3.1 CMIP6 historical simulations. *Geosci. Model Dev.*, **13**, 6383–6423, https://doi.org/10.5194/gmd-13-6383-2020.

Parde, A. N., S. D. Ghude, N. G. Dhangar, P. Lonkar, S. Wagh, G. Govardhan, M. Biswas, and R. K. Jenamani, 2022: Operational probabilistic fog prediction based on Ensemble Forecast System: A decision support system for fog. *Atmosphere*, **13**, 1608, https://doi.org/10.3390/atmos13101608.

Sahu, S. K., G. Beig, and N. S. Parkhi, 2011: Emissions inventory of anthropogenic $PM_{2.5}$ and PM_{10} in Delhi during Commonwealth Games 2010. *Atmos. Environ.*, **45**, 6180–6190, https://doi.org/10.1016/j.atmosenv.2011.08.014.

Salem, M., A. Bose, B. Bashir, D. Basak, S. Roy, I. R. Chowdhury, A. Alsalman, and N. Tsurusaki, 2021: Urban expansion simulation based on various driving factors using a logistic regression model: Delhi as a case study. *Sustainability*, **13**, 10805, https://doi.org/10.3390/su131910805.

Smith, D. K. E., S. R. Dorling, I. A. Renfrew, A. N. Ross, and C. Poku, 2023: Fog trends in India: Relationships to fog type and western disturbances. *Int. J. Climatol.*, **43**, 818–836, https://doi.org/10.1002/joc.7832.

——, and Coauthors, 2024: Forecasts of fog events in northern India dramatically improve when weather prediction models include irrigation effects. *Commun. Earth Environ.*, **5**, 141, https://doi.org/10.1038/s43247-024-01314-w.

Smith, R. N. B., 1990: A scheme for predicting layer clouds and their water content in a general circulation model. *Quart. J. Roy. Meteor. Soc.*, **116**, 435–460, https://doi.org/10.1002/qj.49711649210.

Theethai Jacob, A., and Coauthors, 2023: Implementation of the urban parameterization scheme in the Delhi model with an improved urban morphology. *Quart. J. Roy. Meteor. Soc.*, **149**, 40–60, https://doi.org/10.1002/qj.4382.

Thiery, W., and Coauthors, 2020: Warming of hot extremes alleviated by expanding irrigation. *Nat. Commun.*, **11**, 290, https://doi.org/10.1038/s41467-019-14075-4.

Tiwari, A., V. K. Soni, C. Jena, A. Kumar, S. Bist, and R. Kouznetsov, 2022: Pre-operational validation of Air Quality Forecasting Model SILAM for India. *J. Pollut. Eff. Control*, **10**, 343, https://doi.org/10.35248/2375-4397.22.10.343.

van Weverberg, K., C. J. Morcrette, I. Boutle, K. Furtado, and P. R. Field 2021: A bimodal diagnostic cloud fraction parameterization. Part I: Motivating analysis and scheme description. *Mon. Wea. Rev.*, **149**, 841–857, https://doi.org/10.1175/MWR-D-20-0224.1.

Wang, H., and Coauthors, 2023: Increased night-time oxidation over China despite widespread decrease across the globe. *Nat. Geosci*., **16**, 217–223, https://doi.org/10.1038/s41561-022-01122-x.

Wesely, M. L., 1989: Parameterization of surface resistances to gaseous dry deposition in regional-scale numerical models. *Atmos. Environ.*, **23**, 1293–1304, https://doi.org/10.1016/0004-6981(89)90153-4.

Willmott, C. J., 1981: On the validation of models. *Phys. Geogr.*, **2**, 184–194, https://doi.org/10.1080/02723646.1981.10642213.

Wilson, D. R., and S. P. Ballard, 1999: A microphysically based precipitation scheme for the UK Meteorological Office unified model. *Quart. J. Roy. Meteor. Soc*., **125**, 1607–1636, https://doi.org/10.1002/qj.49712555707.

Woodward, S., 2001: Modeling the atmospheric life cycle and radiative impact of mineral dust in the Hadley Centre climate model. *J. Geophys. Res.*, **106**, 18155–18166, https://doi.org/10.1029/2000JD900795.

Zhang, L., S. Gong, J. Padro, and L. Barrie, 2001: A size-segregated particle dry deposition scheme for an atmospheric aerosol module. *Atmos. Environ.*, **35**, 549–560, https://doi.org/10.1016/S1352-2310(00)00326-5.